ANZIAM J. 43(2001), 149–163

INITIATION OF COMBUSTION WAVES IN SOLIDS, AND THE EFFECTS OF GEOMETRY

J. BRINDLEY[1], J. F. GRIFFITHS[2], A. C. MCINTOSH[3] and J. ZHANG[2]

(Received 30 November, 1998; revised 20 April, 1999)

Abstract

In a recent paper Weber *et al.* [9] examined the propagation of combustion waves in a semi-infinite gaseous or solid medium. Whereas their main concern was the behaviour of waves once they had been initiated, we concentrate here on the initiation of such waves in a solid medium and have not examined in detail the steadiness or otherwise of the waves subsequent to their formation. The investigation includes calculations for finite systems. The results for a slab, cylinder and sphere are compared.

Critical conditions for initiation of ignition by a power source are established. For a slab the energy input is spread uniformly over one boundary surface. In the case of cylindrical or spherical symmetry it originates from a cylindrical core or from a small, central sphere, respectively. The size of source and reactant body is important in the last two cases. With the exception of the initial temperature distribution, the equations investigated are similar in form to those of Weber *et al.* [5, 9] and, as a prelude to the present study, with very simple adaptation, it has been possible to reproduce the results of the earlier work. We then go on to report the result of calculations for the initiation of ignition under different geometries with various initial and boundary conditions.

1. Introduction

There is an inherent industrial problem associated with the processing of powders, whereby combustion may be initiated at hot spots created by friction in equipment such as screw feeders, blenders or valves commonly used in powder handling industries [7]. The issue is not solely that of destruction and loss of a valuable product, but also that ignition of the material may become the source of an explosion in potentially flammable gases either emitted from the material or surrounding it from another source.

[1]School of Mathematics, Leeds University, Woodhouse Lane, Leeds, LS2 9JT, UK.
[2]School of Chemistry, Leeds University, Woodhouse Lane, Leeds, LS2 9JT, UK.
[3]Department of Fuel and Energy, Leeds University, Woodhouse Lane, Leeds, LS2 9JT, UK.

Though an extensive literature has accumulated over recent years [4, 6, 8, 10, 11], there has as yet been no rigorous identification of the conditions in the solid under which ignition may be brought about. The fundamental problem associated with all practical cases is that of a heat flux localised in a very small volume within the mass of reactive material. Energy could be supplied over a comparatively long period or there could be transient dissipation. The source itself may attain a high local surface temperature, certainly far in excess of that which is characterised as the spontaneous ignition temperature of the substance. There would then be local destruction around the hot spot. However a crucial question to answer concerns the circumstances in which a self-propagating combustion wave may break away from the reactive region local to the source. This does not constitute the classical form of criticality, but such a distinction of non-propagation/propagation would arise if the energy flux from the hot spot is appreciably lower than that of the chemical source term for the initiated reaction, as is normally expected to be the case. That is, the source itself is not influential at more remote locations within the reactant. This behaviour has been demonstrated in recent work by Mercer and Weber [5].

In the present paper we address numerically the conditions for the initiation of a combustion wave from a source at constant heat flux. The criteria associated with the three geometries, the slab, the cylinder and the sphere, have been investigated. Both the cylinder and the sphere require a defined dimension to represent the size of the source (or the source relative to the overall size). There is no related physical dimension for a heat flux supplied to one surface of a slab, but the results for the three shapes may be unified if the source is defined as a flux rather than a power dissipation. The sphere represents the closest approach to most practical applications.

The classical assumption of "zero order reaction" or "no reactant consumption" represents another simplifying extreme, but the most interesting behaviour emerges in conditions where reactant depletion is taken into account. Reactant consumption also poses an interesting possibility for the initial conditions that may be adopted in numerical calculations. The natural starting point would be that of material at the temperature set by the outer boundary, with power dissipation beginning at zero time. However, an alternative and illuminating "numerical experiment" is to regard the initial, distributed temperature of the system to be that which would have been established by the continuous energy flux into inert material of the same thermal properties as the reactant. The numerical solution to this rather assumed initial condition in the reactive substance is practically interesting because it may have some bearing on approximate methods which could be used to seek analytical forms to ignition criteria [12]. We explore also the practical question concerning whether or not a combustion wave can be aborted if the power supply is stopped in sufficient time.

The important distinctions of the present set of equations representing the development of a combustion wave compared to the circumstances which may prevail in

practice, are that very often gaseous products may be formed and that oxygen may be required to sustain the reaction. Not only are more complex mathematical descriptions then required but also the predictions from the simple model can be anomalous in practice. For example, the intervention of oxygen is likely to impose a diffusion control on the reaction rate once a combustion wave develops, which will then yield quite different rates of propagation from those predicted in its absence. The equations for mass and energy conservation are developed in dimensionless form, and the merits of non-dimensionalisation are discussed. However, the numerical values for some of the parameters selected in the calculations relate to laboratory scale experiments, specifically a structure of minimum dimension of 5 cm.

2. The model and non-dimensionalisation

The system of reaction-diffusion equations may ne expressed in the form

$$\rho c_p \frac{\partial T}{\partial t} = X Q A e^{-E/RT} + \lambda \left[\frac{\partial^2 T}{\partial r^2} + \frac{j}{r} \frac{\partial T}{\partial r} \right], \tag{1}$$

$$\frac{\partial X}{\partial t} = -X A e^{-E/RT}, \tag{2}$$

where $T \equiv T(r, t)$ represents the temperature and $X \equiv X(r, t)$ the solid fuel density, r and t being the spatial and time co-ordinates. We assume for simplicity that the physical properties, ρ, c_p and λ, of the reactant are independent of temperature and of position, and that the reaction product is also solid with the same physical properties as the reactant. The geometry parameter j takes the value 0, 1 and 2 for the infinite slab, the infinite cylindrical annulus and spherical shell, respectively. The reaction is assumed to be first order exothermic in a single reactant. This is often used in thermal ignition theory, and is the assumption in the work by Weber *et al.* [9]. For the purposes of reaction in solids, the rate of heat release is considered to be proportional to the reactant density.

The boundary conditions are

$$-\lambda \frac{\partial T}{\partial r} = \tilde{P} \text{ at } r = r_0 \qquad \text{and} \qquad -\lambda \frac{\partial T}{\partial r} = h_a (T - T_a) \text{ at } r = r_1,$$

where $\tilde{P}$ is the incoming heat flux (W m^{-2}), T_a is the ambient temperature and h_a the heat transfer coefficient at the exposed surface. We shall assume $h_a = \infty$ (infinite Biot number at the edge), that is, $T|_{r=r_1} = T_a$. In the case of $j = 0$, the one dimensional infinite slab, $r_0 \equiv 0$ and r_1 is the thickness of the slab. In the two other cases r_0 and r_1 are the radii of the the inner and outer surface of the reactant, respectively. The initial

https://doi.org/10.1017/S1446181100011482 Published online by Cambridge University Press

temperature throughout the system is assumed to be uniform and equal to T_a, except where otherwise specified. Thus formally we take

$$X(r, 0) = \rho \qquad \text{and} \qquad T(r, 0) = T_{ini}(r),$$

where $T_{ini}(r) = T_a$ in most cases.

Using the dimensionless variables $u = RT/E$ and $x = X/\rho$, and the co-ordinates $\xi = r/r_n$ and $\tau = t/t_n$, where r_n and t_n are some characteristic scales to be defined, we transform (1) and (2) to

$$\frac{\partial u}{\partial \tau} = x\frac{QARt_n}{c_p E}e^{-1/u} + \frac{\lambda t_n}{\rho c_p r_n^2}\left(\frac{\partial^2 u}{\partial \xi^2} + \frac{j}{\xi}\frac{\partial u}{\partial \xi}\right), \tag{3}$$

$$\frac{\partial x}{\partial \tau} = -x t_n A e^{-1/u}. \tag{4}$$

There are numerous choices for the *characteristic* length and time r_n and t_n. If both the diffusion coefficient and the product $(t_n A)$ are required to be unity then we obtain $r_n = \sqrt{\lambda/\rho c_p A}$ and $t_n = 1/A$. In this case (3) and (4) then become

$$\frac{\partial u}{\partial \tau} = qxe^{-1/u} + \nabla^2 u, \tag{5}$$

$$\frac{\partial x}{\partial \tau} = -xe^{-1/u}, \tag{6}$$

where $q = QR/c_p E$ is the dimensionless adiabatic temperature excess. A slightly different dimensionless form is used by Weber *et al.* [9], such that the parameter β in their equations is equal to q^{-1} in the present paper.

The dimensionless boundary conditions are

$$-\frac{\partial u}{\partial \xi} = \alpha \text{ at } \xi = \xi_0 \qquad \text{and} \qquad u = u_a \text{ at } \xi = \xi_1, \tag{7}$$

where

$$\xi_0 = \frac{r_0}{r_n}, \quad \alpha = \frac{\tilde{P}Rr_n}{\lambda E}, \quad \xi_1 = \frac{r_1}{r_n} \qquad \text{and} \qquad u_a = \frac{T_a R}{E}.$$

The merit of this choice of non-dimensionalisation is that, as far as the reaction-diffusion equations are concerned, different systems are distinguished by a single parameter q. To describe the system completely, 5 independent parameters q, ξ_0, ξ_1, α, and u_a, are required. However, the additional parameters occur only in the boundary conditions.

2.1. Calculations and parameter choices The system of parabolic partial differential equations (5)–(6) was solved numerically using the NAG library routine D03 PBF.

https://doi.org/10.1017/S1446181100011482 Published online by Cambridge University Press

It was found necessary to have about 1000 nodes in the spatial coordinate in order to get accurate results for a 5 cm slab. Since D03 PBF allows fixed nodes, we chose to distribute spatial mesh-points uniformly. The step size of time used in the integration is controlled by a tolerance parameter for the estimate of local error. Usually a tolerance value of 10^{-8} was small enough to ensure accurate results but, occasionally, a value as small as 10^{-10} was required. As the calculation could be very time consuming with small meshes in either the spatial or time coordinate, we used the largest possible step size without incurring significant numerical errors. To ensure that there were no spurious results, a convergence test was always carried out for a new set of input parameters.

The kinetic parameters we used in this work were as follows: $A = 1.0 \times 10^5$ s^{-1}, $Q = 5.7 \times 10^5$ Jkg^{-1}, $E = 8.4 \times 10^4$ Jmol^{-1}. The physical parameters of the reactant and product were $\rho = 660$ kgm^{-3}, $c_p = 750$ Jkg^{-1}K^{-1} and $\lambda = 0.10$ Wm^{-1}K^{-1}. These gave $r_n = 1.43 \times 10^{-6}$ m, $t_n = 1.0 \times 10^{-5}$ s and $q = 0.075$. This q value gives $\beta = 13.3$ and corresponds to the unstable regime described by Weber *et al.* [9] in the semi-infinite slab case. The size of the system was specified by $r_0 = 5$ mm and $r_1 = 5$ cm, or $\xi_0 = 3.5 \times 10^3$ and $\xi_1 = 3.5 \times 10^4$. The ambient temperature was $T_a = 300$ K, giving $u_a = 0.0298$. The initial uniform temperature was the same as the ambient temperature, that is, $u(\xi, 0) = u_a$.

3. Numerical results

3.1. Criticality in a spherical shell Although these results are presented in dimensionless terms, the reaction system comprises a spherical shell of 5 cm radius, within which a power source of 5 mm in radius is buried at the centre. The source and the reactant are regarded as being in perfect thermal contact. Two patterns of behaviour are predicted, which are distinguished as subcritical or supercritical reactions, near a critical heat flux. The distinction in response is characterised by examination of the position of a combustion (ignition) front. The concept of a combustion front is clear in an infinite system because it can be identified as a stationary wave. In a finite system the concept of a combustion front has to be approximate, and the definition is somewhat arbitrary. For present purposes we define it to be where the fuel density is half of the initial value, denoted by $\xi_h \equiv \xi_h(\tau)$. The temperature at ξ_h is termed $u_h \equiv u_h(\tau)$. How these relate to the overall development is shown in examples of subcritical ($\alpha = 1.43845 \times 10^{-5}$) and supercritical ($\alpha = 1.43846 \times 10^{-5}$) behaviour (Figures 1 and 2, respectively). In this case a dimensionless critical flux is identified to be $\alpha^* = 1.43846 \times 10^{-5}$. A critical flux is predicted also for the cylindrical annulus and the slab, and similar patterns are found to develop in either subcritical or supercritical cases.

https://doi.org/10.1017/S1446181100011482 Published online by Cambridge University Press

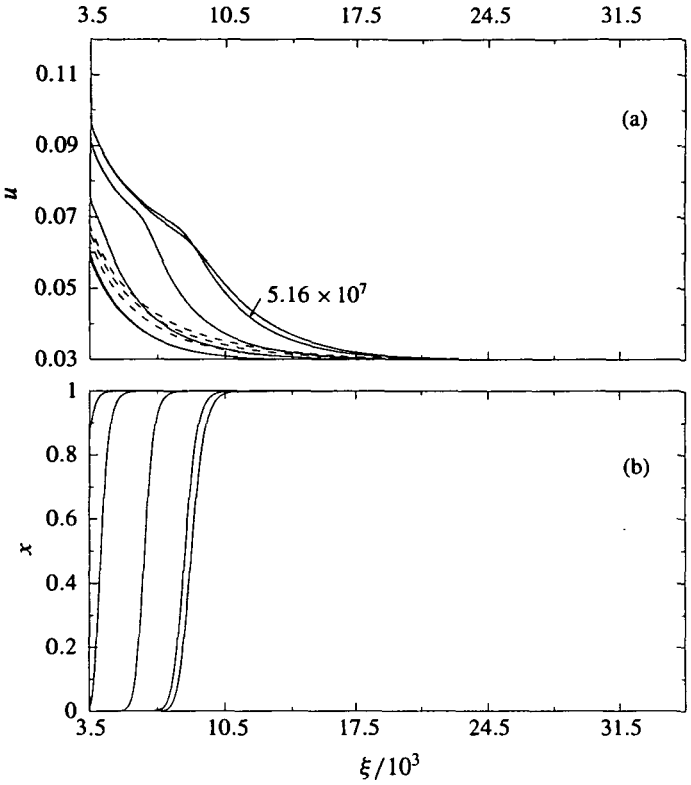

FIGURE 1. Subcritical behaviour of a spherical shell: $j = 2$, $q = 0.075$, $\xi_0 = 3.5 \times 10^3$, $\xi_1 = 3.5 \times 10^4$, $u_a = 0.03$, $\alpha = 1.43845 \times 10^{-5}$, $u_{ini}(\xi) = u_a$. (a) Dimensionless temperature profiles at $\tau = (0, 1.2, 2.4, 3.6, 4.8, 5.16) \times 10^7$. Dashed lines are results of the inert case at $\tau = (1.2, 2.4, 3.6, 4.8) \times 10^7$; (b) Dimensionless reactant density profiles at $\tau = (0, 1.2, 2.4, 3.6, 4.8, 5.16) \times 10^7$.

Switching on the power from cold, that is, $u_{ini}(\xi) = u_a$, causes the surface to heat quickly and energy to be dissipated into the sphere (Figures 1 and 2). For both subcritical and supercritical conditions there is an accompanying reactant consumption, such that the local temperature becomes enhanced quite considerably above that which would be reached in the same time interval under non-reactive conditions (dashed lines in Figure 1).

The distinction between the marginally subcritical and supercritical behaviour is clearly seen in Figures 1 and 2. Similar extents of reaction (and heat release) occur during the early development of the reaction up to $\tau = 4.8 \times 10^7$. However, in the subcritical case the spatial evolution of reaction is driven essentially by local heating as a result of thermal transport from the source through the reacted zone. The decay of the temperature profile and the arresting of the reactant consumption development after $\tau = 5.2 \times 10^7$ can be seen in Figure 1 (also see Figure 3 (a)).

https://doi.org/10.1017/S1446181100011482 Published online by Cambridge University Press

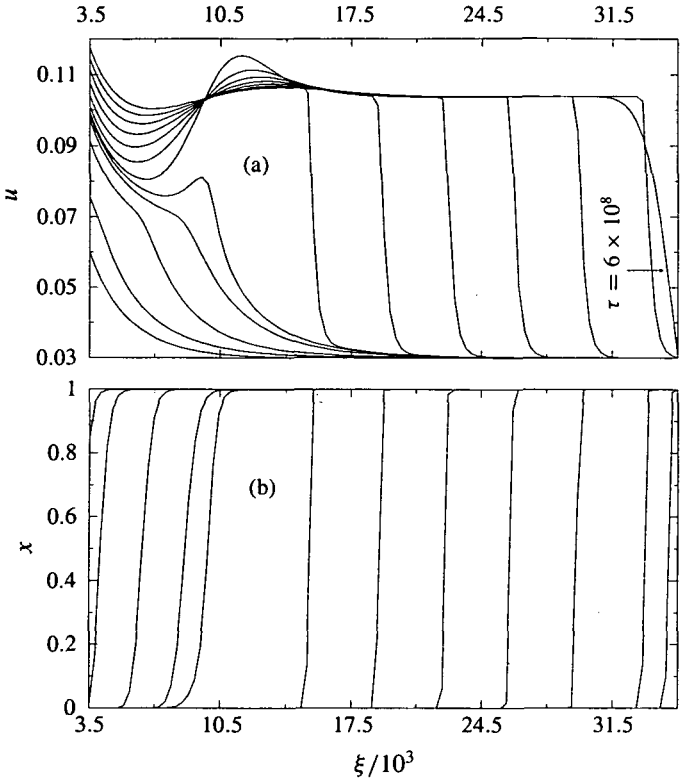

FIGURE 2. Supercritical behaviour of a spherical shell. Parameters are the same as in Figure 1 but $\alpha = 1.43846 \times 10^{-5}$. (a) Dimensionless temperature profiles at $\tau = (0, 1.2, 2.4, 3.6, 4.8, 5.16, 5.28, 5.4, 5.52, 5.64, 5.76, 5.88, 6.0) \times 10^7$; (b) Dimensionless reactant density profiles at the above times.

By contrast, under supercritical conditions an accelerating, self-sustained combustion front begins to develop after $\tau = 4.8 \times 10^7$. In fully dimensional terms it begins at a radius about 0.75 cm greater than that of the surface of the source. This front propagates almost, but not quite, to the edge of the system, where it is extinguished by thermal losses at the surface boundary layer. The rate of heat release and the rate of propagation throughout most of the travel are sufficiently fast that an adiabatic temperature rise occurs in the combustion front. The maximum in the dimensionless temperature at $\xi = 1.3 \times 10^4$ arises from the superposition of $\Delta u_{ad} \approx q$ on the local temperature already imposed by the combined effects of chemical heat release and thermal conduction. That complete reaction has occurred when the maximum temperature is attained, can be seen in the accompanying dimensionless fuel density profile (Figure 2(b)). The local maximum in u gradually decays as a result of the conduction of heat into the trough that exists in the reacted material closer to the hot source. (This decay is consistent with a Fourier time $t_F = 123$ s, assuming that the

https://doi.org/10.1017/S1446181100011482 Published online by Cambridge University Press

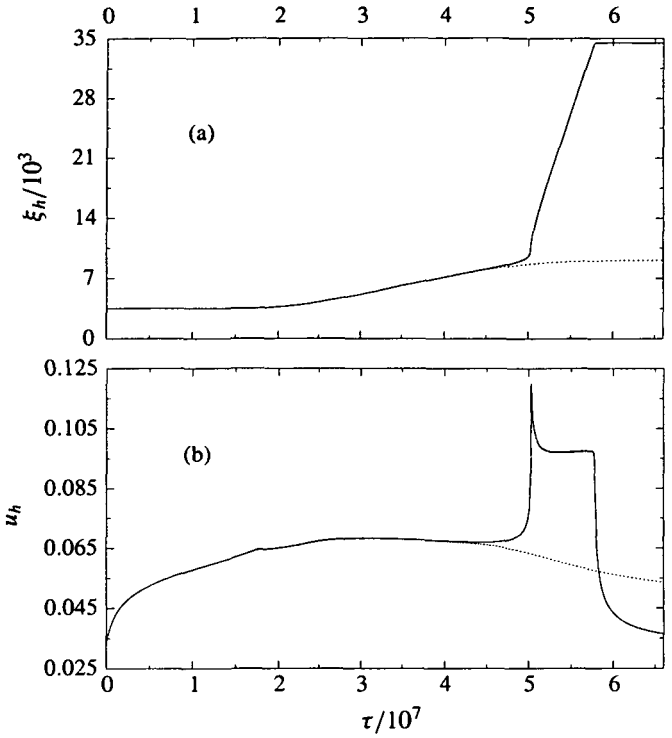

FIGURE 3. Distinction between the subcritical and supercritical cases. Solid and dashed lines correspond to $\alpha = 1.43845 \times 10^{-5}$ (subcritical case shown in Figure 1) and $\alpha = 1.43846 \times 10^{-5}$ (supercritical case shown in Figure 2), respectively. (a) Dimensionless half-density position ξ_h (combustion front) as a function of dimensionless time τ; (b) Dimensionless temperature at the combustion front u_h as a function of τ.

dissipation is from a region of thickness 0.5 cm.)

Both the subcritical and supercritical results, represented by the dotted and solid lines, are summarised in Figure 3 with respect to the dimensionless half-density position (the location of the combustion front) and the dimensionless temperature at such position as a function of dimensionless time. These results show the marked acceleration in the propagation rate and in the temperature change as the combustion wave breaks away. The peak shown in Figure 3 (b) is due to the fact that, just after take-off, the combustion front moves away quickly into the colder region.

3.2. Critical heat flux In this paper we seek to address the following underlying questions related to the initiation of a combustion front: (i) How does the critical flux depend on the thickness of the reactant? (ii) How does the critical flux depend on geometry such as the radius of the source in a cylinder or sphere? (iii) How is the critical flux affected by the initial conditions or by reactant consumption? (iv) Can

https://doi.org/10.1017/S1446181100011482 Published online by Cambridge University Press

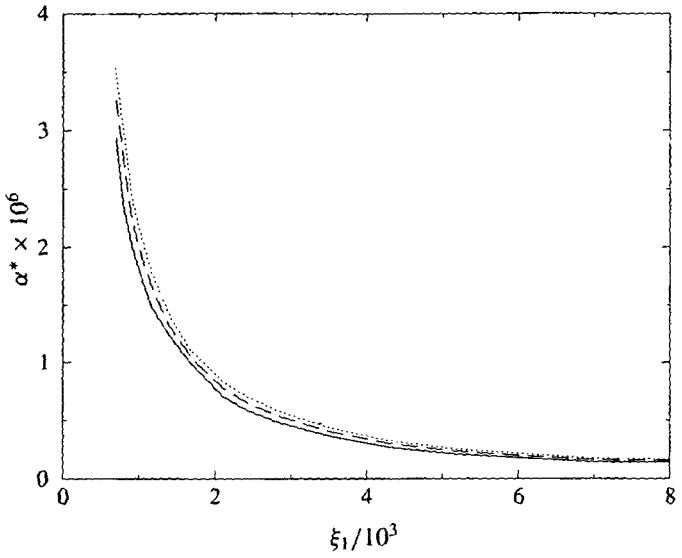

FIGURE 4. Variation of critical heat flux with reactant size ξ_1 in a slab: $j = 0$, $q = 0.075$, $u_a = 0.03$. (a) First order reaction with $u_{int}(\xi) = u_a$ (dotted line); (b) First order reaction with $u(\xi) = u_a + \alpha(\xi - \xi_1)$ (dashed line); (c) Zeroth order reaction (solid line).

a propagating combustion front be aborted if the (supercritical) flux is stopped in sufficient time?

In the interest of simplicity we have assumed a constant heat flux. Though this is a somewhat unrealistic physical problem, it is clear from the character of the results that once the appropriate condition for a combustion wave initiation has been attained, the further progress of the wave is independent of the detail of its *birth*. This is borne out clearly by the results obtained when the heat source is switched off after a finite time, which may be regarded as an extreme simplification of the gradual reduction of heat flux with surface temperature increase which may be expected in a real physical situation.

Calculations have been performed for three different circumstances to address how the critical flux at $\xi = \xi_0$ varies with ξ_1 in order to try and go some way to addressing these questions. The results are shown using non-dimensionalised variables for the slab, the cylindrical annulus and the sphere in Figures 4–6, respectively. The conditions relate to (a) a first order exothermic reaction with $T(r, 0) = T_{inj}(r)$, (dotted lines), (b) a first order exothermic reaction with the initial temperature given by the steady state inert temperature profile at the given heat flux (dashed lines), and (c) a zeroth order (without reactant consumption) exothermic reaction (solid lines).

For each of the geometries, the lowest critical heat flux is required at a given size when no reactant consumption is taken into account. The critical power becomes

https://doi.org/10.1017/S1446181100011482 Published online by Cambridge University Press

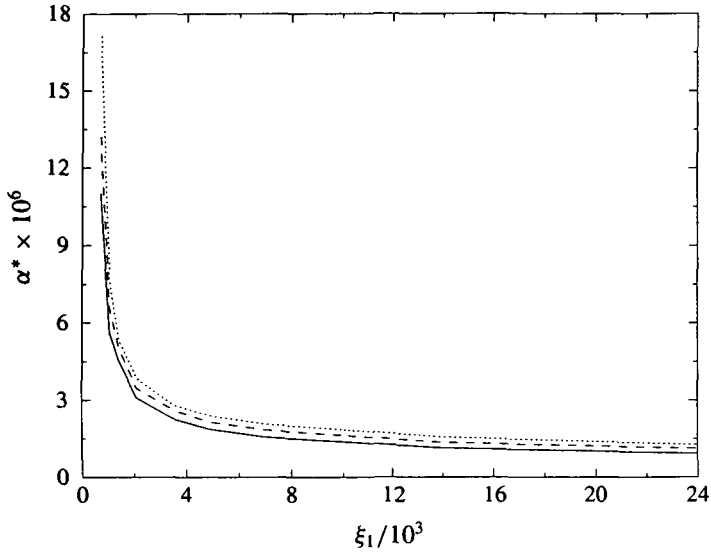

FIGURE 5. Variation of critical heat flux with reactant size ξ_1 in a cylindrical annulus: $j = 1$, $q = 0.075$, $\xi_0 = 3.5 \times 10^3$, $u_a = 0.03$. (a) First order reaction with $u_{int}(\xi) = u_a$ (dotted line); (b) First order reaction with $u(\xi) = u_a + \alpha\xi_0 \log(\xi_1/\xi)$ (dashed line); (c) Zeroth order reaction (solid line).

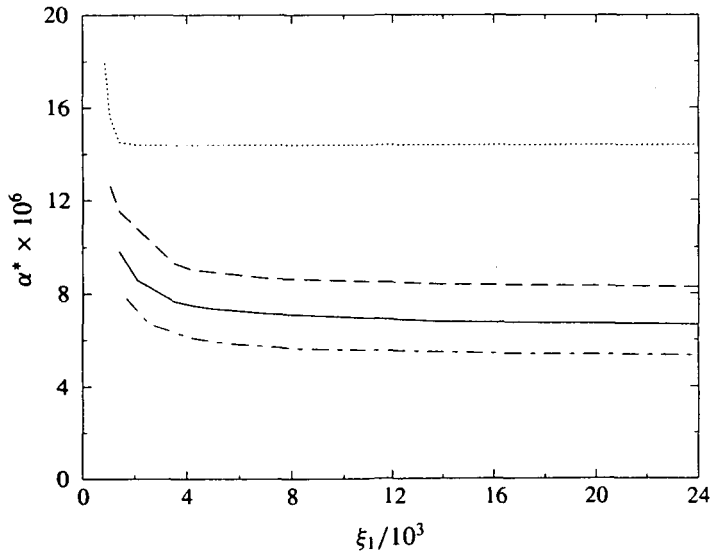

FIGURE 6. Variation of critical heat flux with reactant size ξ_1 in a spherical shell: $j = 2$, $q = 0.075$, $u_a = 0.03$. (a) First order reaction with $u_{int}(\xi) = u_a$, $\xi_0 = 3.5 \times 10^3$, (dotted line); (b) First order reaction with $u_{int}(\xi) = u_a + \alpha\xi_0^2(1/\xi - 1/\xi_1)$, $\xi_0 = 3.5 \times 10^3$ (dashed line); (c) Zeroth order reaction, $\xi_0 = 3.5 \times 10^3$ (solid line); (d) Zeroth order reaction, $\xi_0 = 4.2 \times 10^3$ (dash-dotted line).

https://doi.org/10.1017/S1446181100011482 Published online by Cambridge University Press

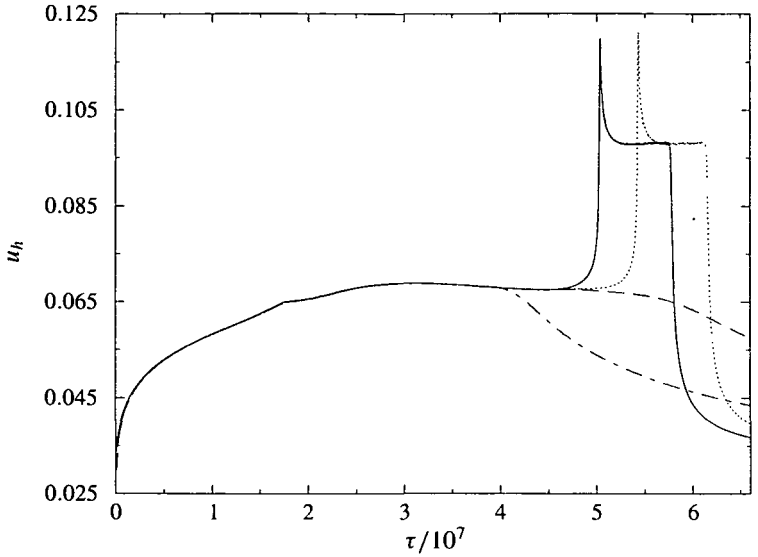

FIGURE 7. Dimensionless temperature at the combustion front (half-density position) as a function of dimensionless time for different stopping time τ_s. Dash-dotted, dashed, dotted and solid lines correspond to $\tau_s = (3.9, 4.42, 4.43, 4.7) \times 10^7$. Other parameters are the same as in Figure 2.

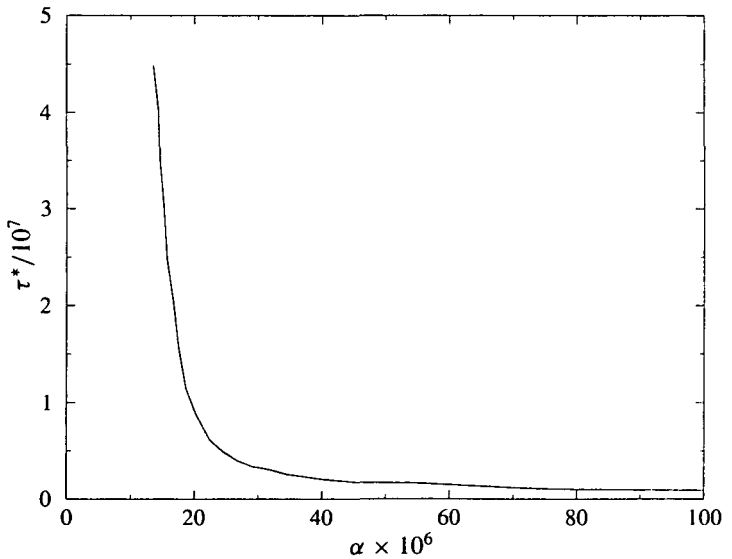

FIGURE 8. Dimensionless critical stopping time τ_s^* as a function of dimensionless heat flux α. Other parameters are the same as in Figure 2.

https://doi.org/10.1017/S1446181100011482 Published online by Cambridge University Press

independent of reactant consumption in very thick slabs, and it does not depend on whether initially the slab is cold or there is an inert profile imposed at the start. There are differences in critical flux between the three cases in thin slabs (Figure 4). Nevertheless, for the slab, the zeroth order case is a reasonable criterion, particularly at large thickness. In the case of the cylindrical annulus the critical flux for the above three conditions are considerably different, but they change with ξ_1 rather similarly. This is not so for the sphere, for which the difference between the first order and zeroth order reactions, and between the first order reaction with different initial temperature profiles are pronounced. An important result for the sphere is that, starting from $u(\xi) = u_a$, even when reactant consumption is taken into account, there is still a point beyond which the critical power appears to become independent of the size of the sphere.

The dependence of critical flux on the radius of the spherical source is included in Figure 6 (dash-dotted line) for the case of zeroth order reaction, when the radius of the source is increased by a factor of 1.2. This result shows that, in the limit of $\xi_1 \gg \xi_0$, the critical flux is not governed merely by the ratio ξ_1/ξ_0. The size of the source itself always remains an independent parameter.

A question has been posed representing a practical circumstance in which the early identification of a heat flux from a source may render the system safe if the heat source is curtailed at a certain time. This situation has been explored in terms of the permitted development of a supercritical condition but with the flux stopped after a prescribed time. Since the energy dissipated in that time is readily determined, there is the basis for transposing to the more general problem in which fixed energies are dumped into a reaction medium at different rates and over a limited interval.

The problem has been addressed with respect to the spherical system described in Subsection 3.1, that is, a 5 mm radius source buried at the centre of a 5 cm radius sphere of reactant. As shown in Figure 7, a second form of criticality is associated with heat flux applied for a limited length of time. In this example, the dashed line represents the development when the power is stopped at $\tau_s = 4.42 \times 10^7$, whereas the dotted line relates to the same power but applied up to $\tau_s = 4.43 \times 10^7$ (a fraction of a second longer in real time). Thus, a critical stopping time $\tau_s^* = 4.43 \times 10^7$ is associated with a flux $\alpha = 1.43846 \times 10^{-5}$. Also shown in the figure are the results of power being stopped at $\tau_s = 3.9 \times 10^7$ (dash-dotted) and $\tau_s = 4.7 \times 10^7$ (solid). The latter case gives a result that is virtually identical to the supercritical behaviour shown in Figure 3 (b), signifying that the propagating combustion front is no longer dependent in any way on the source flux. The critical time is shown in Figure 8 as a function of the heat flux.

https://doi.org/10.1017/S1446181100011482 Published online by Cambridge University Press

4. Discussion and conclusions

By using numerical methods, we have shown how some of the five main parameters associated with the initiation of combustion waves by a constant heat flux affect criticality. Once one moves away from the slab geometry and from the assumption that there is no reactant consumption, the analytical prediction of a critical heat flux to produce a self-sustaining combustion wave is an intractable problem. Clemmow and Huffington [2] obtained solutions for the slab in which there is no reactant consumption, based on the Frank-Kamenetskii exponential approximation [3]. An alternative method, used by Williams [12], is based on a critical Damköhler number to give an analytical prediction of a critical time and temperature profile for ignition. With reactant depletion and non-planar geometry such a Damköhler number approach could not be made without an asymptotic treatment of the thermal boundary layer near the heat source.

The present work differs from that of Weber *et al.* [9] in a number of respects that have been cited in the text. In particular, we have noted that the combustion front does not establish itself as a stationary wave in a finite system with a constant power flux. The propagation is affected by the hot boundary conditions. This means that evidence of chaotic instability of the kind identified by Weber *et al.* [9] cannot be distinguished until the front is very remote from the power source. This is especially acute at high values of β, which signify a low exothermicity of reaction. In calculations of large cylindrical and spherical systems we have distinguished a chaotic propagation remote from the source (at which the systems themselves approximate to planar propagation, as in the case of Weber *et al.* [9]). However, the dimensions selected for the present study do not allow sufficient opportunity for there to be clear evidence of the nature of the instability.

The constant flux condition in a cylinder matches well the problem of electrical power cables or heated pipes surrounded by potentially combustible material. A faulty bearing, which generates a flux through friction, may be approximated as a local source. In this respect also, it may be relevant to perform calculations where the power generation at the source rises linearly with time (mimicking the degradation of a mechanical bearing in a batch mixer, for example). We are proceeding with investigations of a ramped input. It is also our intention to consider the effect of oxygen diffusion into the reacting system, since in most practical cases, oxygen will participate in the reaction. Then it is necessary to include an equation to describe oxygen distribution.

At present in both Weber *et al.* [9] and here fixed nodes are used. To determine the shape of the ignition front and calculate ignition speed more accurately, it may be advantageous to use a numerical integrator that uses a self-adaptive re-meshing technique [1].

Acknowledgement

The authors wish to thank EPSRC in the UK for financial support.

References

[1] M. Berzins, P. M. Dew and R. M. Furzeland, "Developing software for time-dependent problems using the method of lines and differential-algebraic generators", *Appl. Numer. Math.* **5** (1989) 375–397.
[2] D. M. Clemmow and Huffington, "An extension of the theory of thermal explosion and its application to the oscillatory burning of explosives", *Trans. Faraday Soc.* **52** (1956) 385–394.
[3] D. A. Frank-Kamenetskii, *Diffusion and Heat Transfer in Chemical Kinetics*, (transl. by J. P. Appleton), 2nd ed. (Plenum Press, New York, 1969), pp. 374–421.
[4] A. Gomez, G. C. Wake and B. F. Gray, "Frictional and localized heat initiation of ignition: the asymmetrical slab and cylindrical annulus", *Combust. Flame* **61** (1985) 177–187.
[5] G. N. Mercer and R. O. Weber, "Combustion waves in two dimensions and their one-dimensional approximation", *Combust. Theo. Model.* **1** (1997) 157–165.
[6] G. N. Mercer, R. O. Weber, B. F. Gray and S. D. Watt, "Combustion pseudo-waves in a system with reactant consumption and heat loss", *Math. Comput. Model.* **24** (1996) 29–38.
[7] R. L. Rogers and M. A. Nelson, "Ignition of bulk powder by hot spots", *EEC Project: Control and prevention of dust explosion* (1997).
[8] R. O. Weber and G. N. Mercer, "Combustion wave speed", *Proc. R. Soc. Lond.* **A450** (1995) 193–198.
[9] R. O. Weber, G. N. Mercer, H. S. Sidhu and B. F. Gray, "Combustion waves for gases ($Le = 1$) and solids ($Le \to \infty$)", *Proc. R. Soc. Lond.* **A453** (1997) 1105–1118.
[10] R. O. Weber and K. A. Renkema, "Spontaneous ignition in the presence of a power source", *Combust. Sci. Tech.* **21** (1995) 79–83.
[11] R. O. Weber and S. D. Watt, "Combustion waves", *J. Aust. Math. Soc. Series B* **38** (1997) 464–476.
[12] F. A. Williams, *Combustion Theory*, 2nd ed. (Addison Wesley, New York, 1985), p. 285.

A. Appendix: A note on non-dimensionalisation

In the classic Frank-Kamenetskii model for thermal ignition [3], only one parameter, δ, is needed to completely describe a given geometric system. In that sense all systems of the same j value are similar. Therefore the criticality criterion may be readily generalised to different real systems. When the number of independent parameters that define a system of reaction-diffusion equations becomes large, it is very unlikely that two different real systems will be reduced to exactly the same set of dimensionless parameters. Consequently, it is only quite rarely that a dimensionless calculation can serve the purpose of generalising the results to other systems.

It is through non-dimensionalisation that the number of independent parameters is identified for a given system, and a judicious choice helps to show the importance

of the parameter that represents a particular physico-chemical process. However, a simple linear transformation of the form $x' = Kx$, as is invariably used in non-dimensionalisation, does not actually alleviate numerical difficulty in any way. This is because such a linear procedure is merely expansion or contraction of spatial and time coordinates, which is effectively equivalent to an over-all change of temporal or spatial step size used in numerical integration.

In realistic problems, the highest temperature that can be reached in the reactant body is approximately $q + u_{\text{int}} \approx q$, for which usually $0.05 < q < 0.2$. Therefore each of the terms $e^{-1/u}$ and $qe^{-1/u}$ in (5)–(6) in the main text takes a numerical value between 0 and 1, so the equations are, in a sense, *well-behaved*. But the ill-behavedness that arises from high nonlinearity of the original equations (1)–(2) is reflected in the largeness of ξ_1, which may be seen as a measure of the numerical demands of (1)–(2). For kinetic reasons r_n is usually a small quantity, so any realistic system will correspond to dimensionless calculations where very large coordinates are necessary.

Since the value of q does not vary much over a very wide range of reactant in practical situations, the behaviour of different systems will be distinguished principally by size and by the boundary conditions. In particular, the boundary conditions at $\xi = \xi_0$ are a major distinguishing feature of most systems. In many practical cases ξ_0 and ξ_1 take very large values (except in the $j = 0$ case where $\xi_0 \equiv 0$.) Therefore, the critical heat flux at $\xi = \xi_0$ is not strongly sensitive to the actual value of ξ_0 or ξ_1, or to the boundary condition at $\xi = \xi_1$. In such cases, the parameter $\tilde{P}$, which relates to α by $\alpha = \tilde{P}Rr_n/(\lambda E)$, plays the essential role in determining how a system evolves.

https://doi.org/10.1017/S1446181100011482 Published online by Cambridge University Press